Available online at www.sciencedirect.com
SCIENCE DIRECT®
ELSEVIER
Nuclear Instruments and Methods in Physics Research B 205 (2003) 643–650
NIM B
Beam Interactions with Materials & Atoms
www.elsevier.com/locate/nimb

Energy releases in the fission of multiply charged C_{60} ions

J. Jensen [a,b,*], H. Zettergren [b], A. Fardi [b], H.T. Schmidt [b], H. Cederquist [b]

[a] *Manne Siegbahn Laboratory, Frescativägen 24, S-104 05 Stockholm, Sweden*
[b] *Department of Physics, Stockholm University, SCFAB, S-106 91 Stockholm, Sweden*

Abstract

We have studied electron-transfer and collision-induced fragmentation processes in collisions between slow highly charged ions and C_{60} molecules. By using a position sensitive detector, located after a time-of-flight spectrometer, we obtain recoil energies of fragments resulting from post-collisional disintegration of multiply charged C_{60} ions. We deduce kinetic energy releases (KERs) for the cases in which multiply charged C_{60} ions emit either a single C_2^+ ion or a neutral C_2-unit. We find that C_{58}^{4+} ions predominately are due to the emission of a neutral C_2 molecule. Model calculations of KER-values resulting from C_{60}^{r+} ions emitting a C_2^+ ion are presented, and compared with the corresponding experimental results for C_{60}^{r+} with $5 \leqslant r \leqslant 9$.

PACS: 34.70.+e; 36.40.Qv; 36.40.Wa
Keywords: Kinetic energy release; Fission; Fullerenes; Highly charged ions

1. Introduction

Highly excited finite systems, like clusters and large biomolecules, can relax in a variety of ways such as by emission of photons [1], electrons [2] or fragmentation by neutral particle emission. Moreover, multiply charged systems may decay via fission reactions ejecting charged rather than neutral fragments in ways which are analogous to nuclear fission. The instabilities and resulting fission of charged cluster have been studied by many groups both experimentally and theoretically [3–8]. Recently, the Rayleigh stability limit was demonstrated experimentally in studies of fission of charged microdroplets [9]. According to the Rayleigh criterium, the Coulomb repulsion within a multiply charged object (molecule, cluster, droplet etc.) leads to fragmentation if the cohesive energy is weaker than the effective repulsive energy. In this context it is, however, also necessary to consider the internal energy before fragmentation. For collisionally excited C_{60} molecular ions, the mobility of the valence electrons and the coupling of electronic and vibrational degrees of freedom are important. The energetics and dynamics of dissociating neutral and charged fullerenes have received considerable attention over the past decade, and different experimental methods have been used for these studies [10]. In particular, the energy deposition in clusters may be studied through the

* Corresponding author. Address: Department of Physics, Stockholm University, SCFAB, S-106 91 Stockholm, Sweden. Fax: +46-8-5537-8601.
E-mail address: jensen@msi.se (J. Jensen).

0168-583X/03/$ - see front matter © 2003 Elsevier Science B.V. All rights reserved.
doi:10.1016/S0168-583X(03)00532-9

analysis of the kinetic energy release (KER) [11–16] in the various dissociation processes, and by investigating the balance in the production of intact and fragmented C_{60} ions.

Slow highly charged ions have proven to be efficient tools for multiple ionisation of large molecules and clusters [17–19]. At low collision energies, electron capture dominates the interaction, and the capture process occurs at large distances. In this way, one may prepare relatively 'cold' multiply charged clusters with rather low internal energies and high stabilities. C_{60} ions have been observed in charge states up to at least 10 [20] after collisions with slow highly charged ions. In collisions with projectiles in lower charge states, the interaction processes are dominated by smaller impact parameters leading to higher target electronic and vibrational excitations. However, the fragmentation patterns obtained from all keV ion collisions with fullerene exhibit certain m/q values also observed with other ionization methods such as photon absorption [21] and electron impact [22]. In all cases one observes: (i) intact C_{60}^{r+} ions, (ii) C_{60-2m}^{r+} ions (due to evaporation processes

$$C_{60-2m}^{r+} \rightarrow C_{60-2m}^{r+} + C_{2m}, \quad m = 1, 2, 3 \ldots, \tag{1}$$

which are known to dominate for $r \leqslant 3$ [11,23,24]), (iii) $C_{60-2m}^{(r-1)+}$ ions (due to asymmetric fission processes

$$C_{60-2m}^{r+} \rightarrow C_{60-2m}^{(r-1)+} + C_{2m}^{+}, \quad m = 1, 2, 3 \ldots, \tag{2}$$

which is usually taken to be dominant for $r > 4$ [11,23,24]) and (iv) C_n^+ ions (due to multi-fragmentation occurring for even larger r [24]).

In this work, we present experimental results on the KERs in $C_{60}^{r+} \rightarrow C_{58}^{(r-1)+} + C_2^+$ fission processes, as measured by means of recoil momentum (energy) analysis of the $C_{58}^{(r-1)+}$ fragment for $r = 5 \rightarrow 9$. Distant Xe^{17+}–C_{60} collisions at 50 keV were used to ionise the C_{60} molecules. Some of these results may be compared with earlier results using two completely different experimental techniques and (partly) different excitation methods (ion or electron impact). In addition, we compare measurements of KERs in neutral C_2-emission processes $C_{60}^{r+} \rightarrow C_{58}^{r+} + C_2$ for $r = 2, 3$ with literature values by Matt et al. [14], finding again good agreement between fragmentation following collision with Xe^{17+}, He^{2+} (the present measurements) and electrons [14]. Finally, the fission results are compared with a simple model calculation assuming C_2^+ and $C_{58}^{(r-1)+}$ to be perfectly conducting spheres of finite radii.

The next section describes the experimental technique and procedure, while Section 3 is devoted to comparisons with other experimental results and various model calculations.

2. Experimental technique and procedure

The highly charged atomic projectiles used in the present study were produced by the 14.5 GHz ECR ion source at the Manne Siegbahn Laboratory in Stockholm. The ions had energies of 3 keV/q and their mass-to-charge ratios were selected with a double focusing analysing magnet. Behind the magnet, the ion beam was collimated before entering the collision chamber, where it crossed a collimated C_{60}-jet, effusing from a small oven at a temperature of about 600 °C (Fig. 1). The interaction region lies in the extraction stage of a linear time-of-flight (TOF) mass spectrometer. Highly charged projectile ions exiting the collision chamber in the $(q - s)+$ charge state (i.e. stabilizing s electrons) were selected by means of a 180° electrostatic cylindrical analyser followed by a position sensitive detector (PSD). A fast signal from the projectile detector triggered a transverse elec-

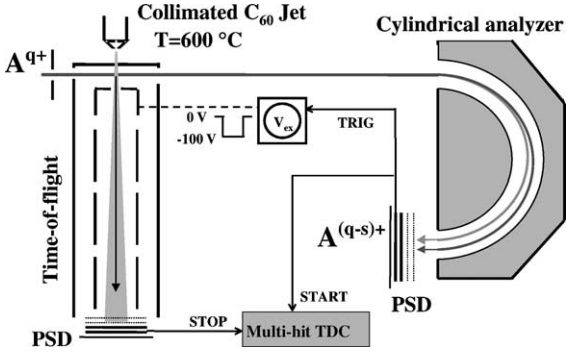

Fig. 1. A schematic of the set-up used for coincidence registration of final projectile and target charge states and the fragment kinetic energies.

tric field, which extracted fullerene recoil ions before entering the drift region of the TOF spectrometer (of length = 1 m), equipped with a PSD (recoil detector with a diameter of 50 mm). The multiply charged fullerenes and their fragments were analysed with respect to their mass-to-charge ratios. The corresponding TOFs were determined by the 'start signals' from the projectile (which also triggered the extraction) and the 'stop signals' from the recoil detector. Note that this method gives a delay – the time it takes the projectile to reach its detector (roughly 1 μs) – between the ionization of a target molecule and its extraction. We used multi-stop detection electronics and the data were stored event by event in list mode.

In Fig. 2 we show the fragmentation patterns of C_{60} recorded in coincidence with outgoing projectiles stabilizing two electrons (s = 2) in collisions with 50 keV Xe^{17+} projectile ions. The target ions were produced in excited states, which decayed by evaporation (1) or asymmetrical fission processes (2). These fragmentation processes were manifested, e.g. in the sequences of peaks to the left of the intact C_{60}^{3+} and C_{60}^{4+} ions.

Events corresponding to one electron stabilized on the projectile (s = 1; not shown here) mostly yield stable (intact) C_{60} ions, due to distant collisions, transfering less energy to the C_{60} molecule than in s = 2 collisions [19,25]. In collisions with more than two electrons stabilized on the projectile (s > 2), hotter C_{60} parent ions are produced and

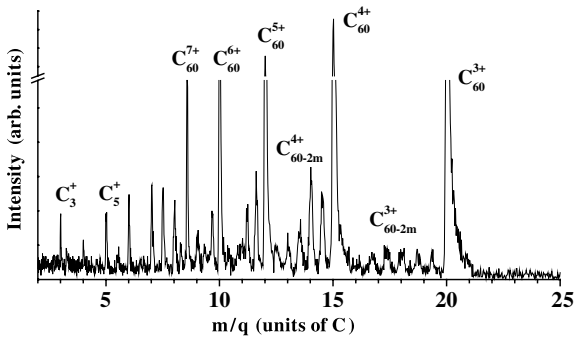

Fig. 2. The fragment distribution of recoiling intact and fragmented C_{60}^{r+} ions measured in coincidence with two stabilized electrons (s = 2) in 50 keV Xe^{17+}–C_{60} collisions. The break on the intensity axis is at 75% of the strongest peak.

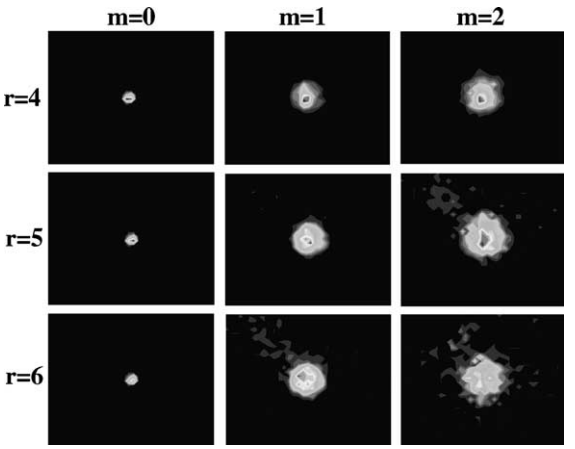

Fig. 3. Position images on the recoil detector for C_{60-2m}^{r+}, $m = 0, 1, 2$ showing KERs in connection with the post-collisional fragmentation of C_{60} following interaction with 50 keV Xe^{17+} ions. The dimensions of the shown detector images are 15×15 mm^2, which are only smaller parts of the whole detector images.

the C_{60} decays through multi-fragmentation yielding larger fractions of smaller carbon clusters. In the present study we have focused on collisions in which two electrons are stabilized on the projectile.

By setting a gate on a certain peak in the TOF spectra, we obtain the corresponding position distribution on the recoil detector. Fig. 3 shows examples of measured distributions for intact and fragmented C_{60}^{r+} ions. In the left row of Fig. 3, the position distributions associated with intact C_{60} ions (C_{60}^{4+} through C_{60}^{6+}) are shown. The widths of the fragment distributions become wider as the fullerene parent charge state, and the numbers of removed C_2-units (simultaneously or sequentially emitted), increase. It is clear that the daughter-ion peaks, C_{58}^{r+}, are broader than their non-dissociative counterparts indicating substantial energy releases in the dissociation processes.

In Fig. 4 we show the projection of the position images on the recoil detector corresponding to C_{60-2m}^{3+} ions for $m = 0 \rightarrow 4$. The widths of the projections increase as the number of emitted C_2-units increases. We have chosen to take the full widths at 22% of the maximum peak heights to represent typical average values of the corresponding KERs [26]. The widths of various C_{60-2m}^{r+}

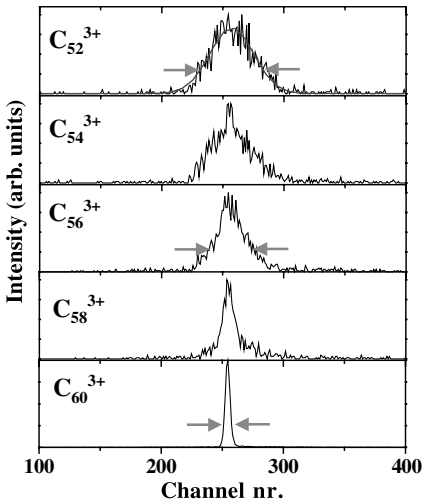

Fig. 4. Projections of the position images on the recoil detector after selecting, in the TOF-spectra, for the peaks corresponding to C_{60-2m}^{3+} ions with $m = 0 \rightarrow 4$.

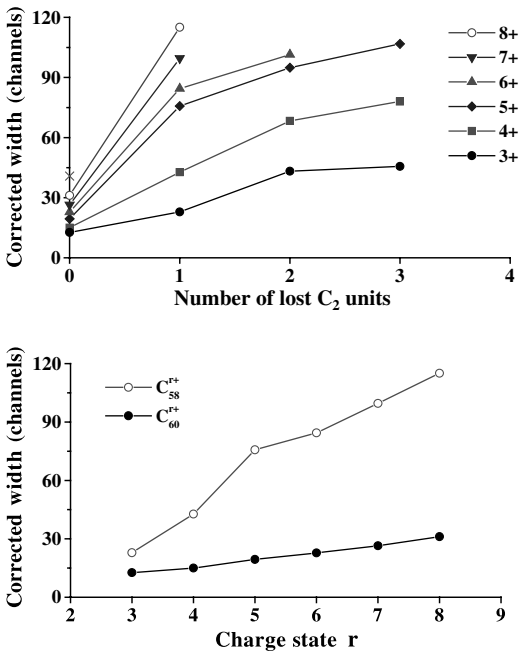

Fig. 5. The full widths at 22% maximum peak heights of projections of C_{60-2m}^{r+} for different numbers of emitted C_2-unit and charge states (above), and of C_{60}^{r+} and C_{58}^{r+} ions for different charge states (below). All widths are scaled to the flight time of C_{60}^{+} (cf. text).

recoil ions are shown in the upper part of Fig. 5 as functions of the numbers, m, of emitted C_2-units. In the lower part of Fig. 5 the widths of intact C_{60}^{r+} ions and C_{58}^{r+} fragment ions are shown. The values in both figures have been corrected for the different flight times of the recoil ions by scaling the measured widths with factors equal to the ratios between the flight times of C_{60}^{+} and the various C_{60-2m}^{r+} recoil ions. Clear differences between the (corrected) widths of intact and fragmented ions, due to the KERs associated with the emission of single C_2-units (charged or neutral), are seen in the lower part of Fig. 5.

From the widths of the fragment ion peaks on the recoil detector, it is possible to deduce the kinetic energy of e.g. C_{58}^{r+} recoils. In order to calibrate the measured widths to kinetic energy scales, Xe-gas was introduced in the interaction region. In Fig. 6 we show a comparison between the position distributions on the recoil detector following single-electron capture from room temperature ($T = 300$ K) Xe gas and the collimated C_{60}-jet. By means of the corresponding (300 K) three-dimensional Maxwellian velocity distribution of Xe we calibrate the fragment kinetic energy scale. The width of Xe^+ corresponds to 40 meV as given by the thermal distribution, while the recoil energy of

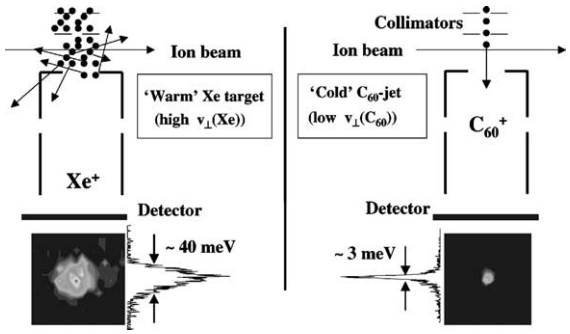

Fig. 6. Schematic picture of the calibration and resolution of our recoil spectrometer. To the left is shown the distribution following single-electron capture from thermal Xe gas (used for calibration). To the right is shown the collimation of the C_{60}-jet, yielding a target with a much lower transversal temperature than in the Xe case.

Xe^+ from the Xe^{17+}+Xe single-electron capture collision easily can be shown to be much smaller. The velocity spread of the collimated C_{60}-jet per-

pendicular to the spectrometer axis can thus be determined to ~3 meV, which is the experimental resolution for the KER measurements. Without this collimation, the transverse temperature of the jet would give a spot size on the recoil detector much larger than that for Xe^+ (due to a longer flight time for C_{60}^+).

3. Results and discussion

From the kinematics of a fragmentation process leading to two fragments the KER is uniquely determined by momentum and energy conservation [30]. In the analysis, the widths of the daughter ions have been corrected (deconvoluted) by the widths of the parent ion, which represents the instrumental broadening and the very narrow energy distributions of the intact C_{60} ions. In Fig. 7 we show the measured KER values for the process where C_{60}^{r+} emits a single C_2^+- or a neutral C_2-unit as a function of the final C_{58}-fragment charge state. This is compared with published and unpublished measurements using different methods such as the mass-analyzed ion kinetic energies (MIKE) and TOF techniques. In the MIKE-scan technique [11–14], the energy distribution of the selected heavy fragments (C_{58}^{r+}) are measured by means of an electrostatic analyzer, and from their

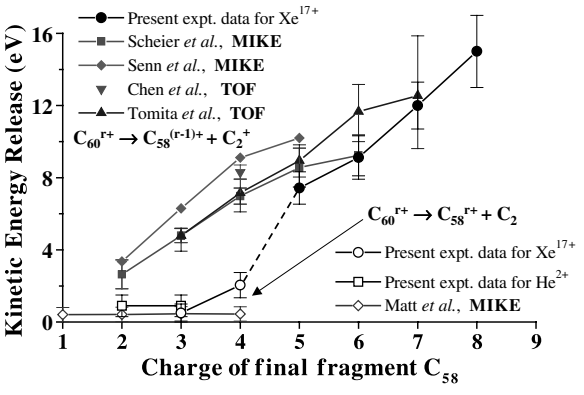

Fig. 7. Measured KERs for the process where C_{60}^{r+} emits a single C_2-unit (charged or neutral) compared with existing measurements based on other methods, such as the MIKE technique by Scheier et al. [11], Senn et al. [13], and Matt et al. [14], and the TOF technique by Chen et al. [15] and Tomita et al. [27].

widths, the KER values are determined [13]. In the TOF technique [15,16,27], the energy distribution of the C_2^+-fragment were obtained from peak shape analysis of the C_2^+-peaks in the TOF spectra. In those measurements, the primary C_{60} ions were produced by slow highly charge ion impact, as in our case, whereas the MIKE-scan measurements used electron impact to ionise the C_{60} molecules.

In the measurements by Scheier [11], Senn [13], Chen [15] and Tomita [27], the experimentally selected dissociation process is that of pure asymmetric fission, of the type given by Eq. (2) for $m = 1$, which dominates for charges of C_{58} larger than four [11,24]. Our values are in good agreement with the fission data in this range, which shows that the present technique gives results consistent with the C_2^+-TOF and the MIKE-scan analysis, and that the KER is governed by the inherent properties of C_{60}^{r+} ions and not by the specific excitation method (ions or electrons). In the measurements of Matt [14], purely evaporative processes of the type given by Eq. (1) are selected (dominating for charges of C_{58} lower than three [11,24]), which yield much lower KER values than fission. In our measurements we see large contributions from evaporation of neutral C_2-units, for final charges of C_{58} ions lower than five. In Fig. 7 we also show KER results for fragmentation after 6 keV He^{2+} impact, consistent with the one obtained with Xe^{+17} impact for C_{58}^{3+} (C_{58}^{2+} was not produced with Xe^{+17} impact). The He^{2+} measurements are also in agreement with the evaporation values measured by Matt [14], within the experimental error bars. These comparisons demonstrate that the present technique is applicable for large and small values of the KERs. The present low KER-value of C_{58}^{4+} ions compared with those obtained for asymmetric fission, suggests that these ions originate predominately from the evaporation of a neutral C_2 from C_{60}^{4+} and not from the fission of C_{60}^{5+}. This is qualitatively in good agreement with the results of Martin et al. [23] and Chen et al. [28], who measured dominance of evaporation over fission for the decay of C_{60}^{4+} produced in fcollisions stabilizing two electrons ($s = 2$) on Ar^{8+}- and Xe^{8+}-projectiles. However, similar measurements using two electron stabilization ($s = 2$) on more highly charged Xe^{30+} projectiles

by Martin et al. [24] yielded a larger preference for C_2^+-emission from C_{60}^{5+}.

For the discussion of the present experimental results, we will use a simple model [5,29] for the interaction between two charged conducting spheres to estimate the KER for C_2^+-emission. We model C_{58} and C_2^+ fragments as metal spheres with the same volume density as the intact C_{60}-ion. This gives

$$a^{\mathrm{H}} = 7.2a_0(1-2m/60)^{1/3},$$
$$a^{\mathrm{L}} = 7.2a_0(2m/60)^{1/3}, \tag{3}$$

where a^{H} and a^{L} are the radii of the heavy and the light fragments, yielding $a^{\mathrm{H}} = 7.1a_0$ and $a^{\mathrm{L}} = 2.3a_0$ for C_{58} and C_2, respectively.

The interaction energy of the two metal spheres is [29]

$$U_{\mathrm{int}}(R) = \frac{1}{2}\left[\frac{q^{\mathrm{H}}(q_0^{\mathrm{H}}-q^{\mathrm{H}})}{a^{\mathrm{H}}} + \frac{q^{\mathrm{L}}(q_0^{\mathrm{L}}-q^{\mathrm{L}})}{a^{\mathrm{L}}}\right], \tag{4}$$

where q^{H} and q^{L} are the net sphere charges, while q_0^{H} and q_0^{L} are the center charges, which are functions of both net charges, the sphere radii and the center–center distance R [29]. In Fig. 8 we show four examples of $U_{\mathrm{int}}(R)$ for $C_{58}^{(r-1)+} + C_2^+$ ($r = 2-5$), where $(r-1) = q^{\mathrm{H}} = 1, 2, 3$ and 4 and $q^{\mathrm{L}} = 1$. The shapes of the curves are due to the strong polarizations (described exactly by infinite sets of image charges [29]) of both spheres at small distances. For larger separations ($R \gg a^{\mathrm{L}} + a^{\mathrm{H}}$), the polarization effect becomes weaker and Eq. (4) approaches the pure Coulomb energy, $q^{\mathrm{H}}q^{\mathrm{L}}/R$.

The present model KERs are taken as the difference between the interaction energy for infinite separation and the maximum of the barrier. The interaction energy is zero when $R = \infty$ and the KER is thus equal to the fusion barrier height. Calculated KER-values for the fission process $C_{60}^{r+} \rightarrow C_{58}^{(r-1)+} + C_2^+$ are shown in Fig. 9 together with experimental results, now as functions of the initial C_{60}^{r+} charge state. Shown are, in addition, calculated energy releases obtained by (i) taking the maximum of the interaction energy between $C_{58}^{(r-1)+}$ (considered to be a charged conducting sphere) and a point charge [13] and (ii) the case for two point charges at the (minimum) distance corresponding to $a^{\mathrm{L}} + a^{\mathrm{H}}$. For low r, it is obviously only important to take the polarization of the large fragment into account, while the effect of the finite radius of the small fragment becomes more important at larger r. However, the differences are fairly small in the region of $r(= 2 \rightarrow 9)$, which we are considering here, but as will be discussed in a forthcoming publication these small differences lead to important differences in the prediction of the stability limit for highly charged C_{60} ions [30].

In the present very simple model it is of course assumed that fission products are in their electronic and vibrational ground states. This is most

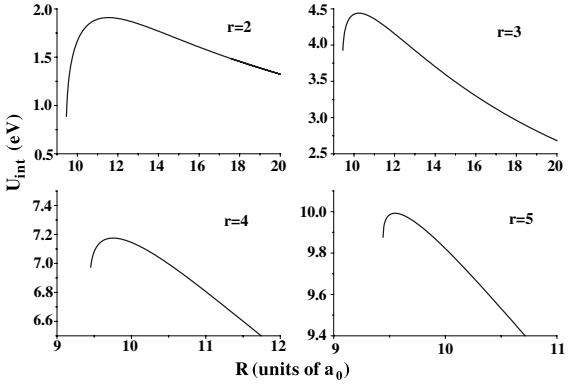

Fig. 8. The interaction energies $U_{\mathrm{int}}(R)$ for two charged spheres modeling the $C_{58}^{(r-1)+} + C_2^+$ interaction as a function of the center–center distances R. Note that $U_{\mathrm{int}}(R = \infty) = 0$ for all cases.

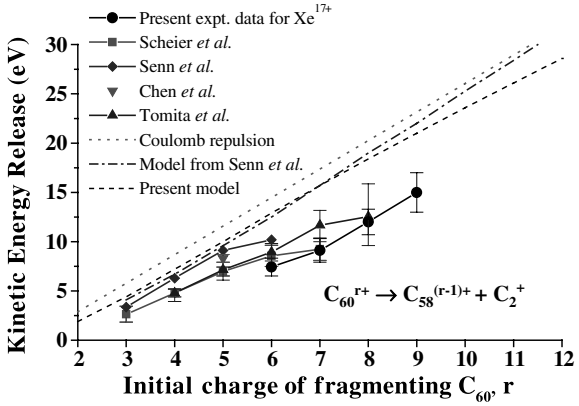

Fig. 9. Measured and calculated KERs for the fission process where a C_{60}^{r+} ion emits a single C_2^+ ion. Three different model results are shown.

likely not the case in the experimental situation, especially since the C_{60}^{r+} ions are excited before fragmentation, partly due to the heating from the oven, and partly due to the collision process. This results in a final excited state with a higher energy yielding a smaller difference in relation to the maximum of the barrier, and thereby smaller KER-values. Keeping in mind that the present model indeed is extremely simple the observed difference between the model and the experiment (Fig. 9), may in principle be explained by the final internal excitations of the fragmentation products.

4. Conclusion and outlook

In the present work, we have presented a new technique to measure KERs in $C_{60}^{r+} \rightarrow C_{58}^{(r-1)+} + C_2^+$ and $C_{60}^{r+} \rightarrow C_{58}^{r+} + C_2$ fragmentation processes. The energy resolution in the measurements of the C_{58}^{r+} fragments is 1 meV as achieved by means of a collimated effusive C_{60}-jet pointing along the axis of a linear TOF spectrometer terminated by a two-dimensional PSD. Experimental results on the fission processes (C_2^+-emission) are in good agreement with other experimental results using quite different experimental techniques. Also, our measurements on C_2-evaporation are found to be in good agreement with earlier results. The measured KERs are found to be significantly lower than estimates using a simple sphere–sphere interaction model to calculate fusion barriers. It is noted that the lower experimental values, in principle, may be explained by internal excitations of the fragments after the dissociation.

Finally, we note that the very narrow initial transverse (to the jet) momentum distribution in the C_{60}-jet may open up possibilities to measure the longitudinal momentum distributions of intact C_{60} ions due to the electron capture process, and thus to deduce the final projectile capture states.

Acknowledgements

This work is supported by the Swedish Natural Research Council through contract no. F650-19981278 and F5102-993/2001 and by The Swedish Foundation for International Cooperation in Research and Higher education (STINT).

References

[1] S. Tomita, J.U. Andersen, C. Gottrup, P. Hvelplund, U.V. Pedersen, Phys. Rev. Lett. 87 (2001) 073401.
[2] J.U. Andersen, P. Hvelplund, S.B. Nielsen, U.V. Pedersen, S. Tomita, Phys. Rev. A 65 (2002) 053202.
[3] U. Näher, S. Frank, N. Malinowski, U. Zimmermann, T.P. Martin, Z. Phys. D 31 (1994) 191.
[4] C. Brechignac, Ph. Cahuzac, F. Carlier, M. de Frutos, R.N. Barnett, U. Landman, Phys. Rev. Lett. 72 (1994) 1636.
[5] U. Näher, S. Bjørnholm, S. Frauendorf, F. Garcias, C. Guet, Phys. Rep. 285 (1997) 245.
[6] S. Krückeberg, G. Dietrich, K. Lützenkirchen, L. Schwiekhard, J. Ziegler, Phys. Rev. A 60 (1999) 1251.
[7] F. Chandezon, S. Tomita, D. Cormier, P. Grübling, C. Guet, H. Lebius, A. Pesnelle, B.A. Huber, Phys. Rev. Lett. 87 (2001) 153402.
[8] L. Chen, S. Martin, R. Brédy, J. Bernard, J. Désesquelles, Europhys. Lett. 58 (2002) 375.
[9] D. Duft, H. Lebius, B.A. Huber, C. Guet, T. Leisner, Phys. Rev. Lett. 89 (2002) 084503.
[10] F. Biasioli, T. Fiegele, C. Mair, G. Senn, S. Matt, R. David, M. Sonderegger, A. Stamatovic, P. Scheier, T.D. Märk, Int. J. Mass. Spectrom. 193 (1999) 267.
[11] P. Scheier, B. Dünser, T.D. Märk, Phys. Rev. Lett. 74 (1995) 3368.
[12] T.D. Märk, P. Scheier, Nucl. Instr. and Meth. B 98 (1995) 469.
[13] G. Senn, T.D. Märk, P. Scheier, J. Chem. Phys. 108 (1998) 990.
[14] S. Matt, M. Sonderegger, R. David, O. Echt, P. Scheier, J. Laskin, C. Lifshitz, T.D. Märk, Int. J. Mass. Spectrom. 185 (1999) 813.
[15] L. Chen, J. Bernard, G. Berry, R. Brédy, J. Désesquelle, S. Martin, Phys. Scr. T 92 (2001) 138.
[16] S. Tomita, H. Lebius, A. Brenac, F. Chandezon, B.A. Huber, Phys. Rev. A 65 (2002) 053201.
[17] B. Walch, C.L. Cocke, R. Voelpel, E. Salzborn, Phys. Rev. Lett. 72 (1994) 1439.
[18] F. Chandezon, C. Guet, B.A. Huber, D. Jalabert, M. Maurel, E. Monnand, C. Ristori, J.C. Rocco, Phys. Rev. Lett. 74 (1995) 3784.
[19] H. Cederquist, A. Fardi, K. Haghighat, A. Langereis, H.T. Schmidt, S.H. Schwartz, J.C. Levin, I.A. Sellin, H. Lebius, B.A. Huber, et al., Phys. Rev. A 61 (2000) 022712.
[20] A. Brenac, F. Chandezon, H. Lebius, A. Pesnelle, S. Tomita, B.A. Huber, Phys. Scr. T 80B (1999) 195.
[21] E.E.B. Campbell, K. Hoffmann, I.V. Hertel, Eur. Phys. J. D 16 (2001) 345.
[22] R. Völpel, G. Hoffmann, M. Steidl, M. Stenke, M. Schlapp, R. Trassl, E. Salzborn, Phys. Rev. Lett. 71 (1993) 3439.

[23] S. Martin, L. Chen, A. Denis, J. Désesquelle, Phys. Rev. A 57 (1998) 4518.
[24] S. Martin, L. Chen, A. Denis, R. Brédy, J. Bernard, J. Désesquelle, Phys. Rev. A 62 (2000) 022707.
[25] A. Langereis, J. Jensen, A. Fardi, K. Haghighat, H.T. Schmidt, S.H. Schwartz, H. Zettergren, H. Cederquist, Phys. Rev. A 63 (2001) 062725.
[26] T. Rauth, O. Echt, P. Scheier, T.D. Märk, Chem. Phys. Lett. 247 (1995) 515.
[27] S. Tomita, H. Lebius, A. Brenac, F. Chandezon, B.A. Huber, Phys. Rev. A (2003), submitted for publication.
[28] L. Chen, J. Bernard, A. Denis, S. Martin, J. Désesquelle, Phys. Rev. A 59 (1999) 2827.
[29] H. Zettergren, H.T. Schmidt, H. Cederquist, J. Jensen, S. Tomita, P. Hvelplund, H. Lebius, B.A. Huber, Phys. Rev. A 66 (2002) 032710.
[30] J. Jensen, H. Zettergren, A. Fardi, H.T Schmidt, H. Cederquist, Phys. Rev. A (2003), submitted for publication.